Journal of Power Sources 248 (2014) 239–245

Contents lists available at ScienceDirect

Journal of Power Sources

journal homepage: www.elsevier.com/locate/jpowsour

Evaluation of Ni/SDC as anode material for dry CH_4 fueled Solid Oxide Fuel Cells

Zhiming Wang [a, b], Yongdan Li [a], Johannes W. Schwank [b, *]

[a] Tianjin Key Laboratory of Applied Catalysis Science and Technology and State Key Laboratory for Chemical Engineering (Tianjin University), School of Chemical Engineering, Tianjin University, Tianjin 300072, China
[b] Department of Chemical Engineering, University of Michigan, 2300 Hayward, Ann Arbor, MI 48109, USA

HIGHLIGHTS

- SOFCs with the configuration of Ni/SDC|SDC|BSCF were prepared and characterized.
- The SOFCs exhibited very good performance in both dry H_2 and CH_4 fuel.
- At 700 °C, the performance in dry CH_4 is better than in H_2.
- Under DEO of CH_4 conditions, the anode shows remarkable resistance to carbon deposition.
- Small amounts of four different carbon species are deposited on the anode.

GRAPHICAL ABSTRACT

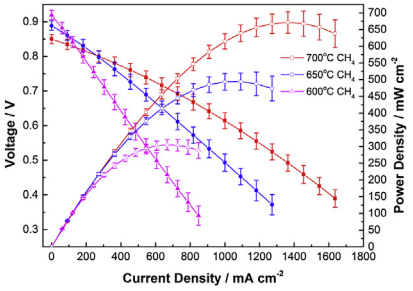

ARTICLE INFO

Article history:
Received 16 June 2013
Received in revised form
7 September 2013
Accepted 10 September 2013
Available online 20 September 2013

Keywords:
Solid oxide fuel cell
Anode
Methane
Electrochemical performance
Ni/SDC

ABSTRACT

A Ni/$Sm_{0.2}Ce_{0.8}O_{1.9}$ (SDC) composite was employed as anode material for direct electrochemical oxidation (DEO) of dry CH_4 in a solid oxide fuel cell. The anodic performance was investigated at temperatures between 600 °C and 700 °C using SDC as electrolyte material and $Ba_{0.5}Sr_{0.5}Co_{0.8}Fe_{0.2}O_{3-\delta}$ (BSCF) as cathode material. The single cell exhibited maximum power densities of 671 mW cm^{-2}, 494 mW cm^{-2} and 305 mW cm^{-2} in dry CH_4 at 700 °C, 650 °C and 600 °C, respectively. Remarkably, at 700 °C the power density in CH_4 was higher than in H_2, thanks to the carbon tolerance of the anode. Durability tests under constant 300 mA output current showed only 3.7% performance loss after 72 h operation. The results demonstrate that Ni/SDC can be used as anode for the DEO of dry CH_4 even at temperatures as low as 600 °C.

© 2013 Elsevier B.V. All rights reserved.

1. Introduction

Solid oxide fuel cells (SOFCs) are electrochemical devices that convert the chemical energy of a combustible fuel directly into electricity. There has been considerable interest in these devices in the past few decades because of their potential for portable power generation, and also for stationary or auxiliary power supply units [1,2]. The high operation temperatures of SOFCs lead to fast reaction kinetics. This allows the utilization of readily available fuels, such as natural gas, coal gas, gasoline, diesel, jet fuel, and even solid carbon [3–7]. A particularly attractive concept is to use these fuels through direct electrochemical oxidation (DEO) without internal or external reforming processes [8,9]. The advantages of this approach are high

* Corresponding author. Tel.: +1 734 764 3374; fax: +1 734 763 0459.
E-mail address: schwank@umich.edu (J.W. Schwank).

0378-7753/$ – see front matter © 2013 Elsevier B.V. All rights reserved.
http://dx.doi.org/10.1016/j.jpowsour.2013.09.043

energy efficiency and relatively simple system design. In addition, commercial hydrocarbon fuels can be safely stored and are more readily available than hydrogen, and this can reduce the overall operation costs [10].

While the concept of the DEO of hydrocarbons into electricity using SOFCs is appealing, there are many operational problems that still need to be solved [1,8,11–14]. The most critical issue is the deactivation of the typical NiO/yttria-stabilized zirconia (YSZ) anode material by carbon deposition [8,11,14]. The typical NiO/YSZ anode material has excellent catalytic properties for fuel oxidation and good electrical conductivity. Ni not only catalyzes the breaking of C–H bonds in hydrocarbons, but also catalyzes the formation of C–C bonds, and this leads to the rapid formation of carbon deposits that can cover the catalytically active Ni sites [15,16]. Moreover, the deposited carbon can block the anode pores, increase gas diffusion resistance and disrupt the anode structure, leading to permanent damage [6].

The formation of carbon deposits can be suppressed by introducing large amounts of steam or carbon dioxide on the anode side to oxidize and remove the carbon deposits [17–19]. However, the introduction of steam or carbon dioxide dilutes the fuel and lowers the energy density. Introduction of steam also results in a highly endothermic steam reforming process. This affects the temperature control, and to heat the steam to operation temperature requires significant additional energy.

Therefore, there is a need for developing new kinds of carbon resistant SOFC anode materials for the DEO of hydrocarbon fuels. Many different strategies have been tried to achieve this goal. Gorte and co-workers investigated rare-earth doped ceria impregnated with CuO as the anode material for direct utilization of hydrocarbon fuels such as CH_4 and gasoline in the SOFC [4,6,20,21]. Their pioneering work demonstrated the feasibility of DEO of CH_4 and other hydrocarbon fuels in SOFC, however, the catalytic activity of this anode material proved to be not high enough. Using alloys is also a promising approach to impart better carbon resistance. For example, Kim et al. [22] tested a Cu–Ni alloy as SOFC anode for direct oxidation of CH_4, and achieved good power density and only moderate carbon deposition. Nikolla et al. [23] used Sn/Ni alloy as anode material for a direct reforming SOFC fed with CH_4 or isooctane. Their results showed that the tolerance of the anode to carbon deposition could be significantly enhanced by introduction of a small amount of Sn to form Sn/Ni surface alloys. Also, some researchers have used anode barrier layers. Lin et al. [24] used a composite of partially stabilized zirconia (PSZ) and CeO_2 as diffusion barrier layer and demonstrated an increase in the stable operating parameter range of Ni–YSZ anode-supported SOFCs that were operated directly with CH_4. There is one other commonly employed strategy, using oxygen-deficient, mixed-valent perovskite materials as anode for their high ionic and electronic conductivity and good electrochemical activity in a reducing atmosphere. Tao and Irvine [25] reported that the perovskite $La_{0.75}Sr_{0.25}Cr_{0.5}Mn_{0.5}O_{3-\delta}$ (LSCM) gave very good performance for DEO of CH_4. However, this material had a low electronic conductivity in reducing atmosphere and relatively low activity [26]. Huang et al. [27–29] investigated a double-perovskite $Sr_2MMoO_{6-\delta}$ (M = Mg, Co, Ni) as SOFC anode material for H_2 and CH_4 fuels. Their results showed that $Sr_2MgMoO_{6-\delta}$ is an excellent SOFC anode material with appreciable stability. Sr_2CoMoO_6 exhibited a high cell performance in H_2 and wet CH_4, while Sr_2NiMoO_6 showed notable power output only in dry CH_4. Li et al. [30,31] used $Sr_2Fe_{1-x}Mo_{1+x}O_6$ for DEO of CH_4 and methanol, and achieved good and stable performance.

However, most of the above-mentioned approaches required high operation temperatures (about 850 °C), resulting in higher systems costs and performance degradation rates, as well as slow start-up and shutdown cycles [32]. In the present work, we introduced a Ni/$Sm_{0.2}Ce_{0.8}O_{1.9}$ (SDC) composite anode for DEO of CH_4 at lower temperature. Thanks to the high oxygen ion conductivity of SDC, the good contact between Ni and SDC, and the relatively low operation temperature, this anode material appeared promising for achieving good and stable performance. We also investigated the extent of carbon deposition on the Ni surface to demonstrate the carbon resistance of this anode. While this work was focused on the DEO performance of the Ni/SDC composite anode when fueled with pure H_2 or CH_4, the insights gained set the stage for future exploration of DEO of natural gas.

2. Experimental

2.1. Material preparation

SDC powder with a composition of $Sm_{0.2}Ce_{0.8}O_{1.9}$ was prepared by an oxalate co-precipitation technique. A proper amount of oxalic acid was dissolved in diluted water to form a 0.5 mol L^{-1} solution. The pH value of the solution was adjusted to around 6.8 by adding $NH_3 \cdot H_2O$. A proper amount of Sm_2O_3 was dissolved in diluted nitric acid, then the desired amounts of $Ce(NO_3)_3 \cdot 6H_2O$ and deionized water were added to form solutions containing 1 mol L^{-1} metal ions (Ce^{3+} and Sm^{3+}). The solution of Ce^{3+} and Sm^{3+} was slowly added into oxalic acid solution to form the oxalate precursor. The mole ratios of oxalic acid, Ce^{3+}, and Sm^{3+} were controlled to be 2.25:0.8:0.2. During the addition, $NH_3 \cdot H_2O$ solution was used to maintain the pH value between 6.6 and 6.9. The resulting precipitate was vacuum-filtrated and washed four times with deionized water, followed by washing with ethanol for three times. Then the precipitate was dispersed in ethanol with ultrasonic treatment for 30 min. The final material was dried at 85 °C overnight, followed by calcination at 750 °C for 2 h to obtain the SDC powder.

To synthesize the anode material, SDC powder and NiO powder (Alfa Aesar) with a weight ratio of 1:1 were mixed thoroughly by ball milling for 24 h. The final calcination procedure for the anode material was carefully controlled to be 1000 °C for 1 h in order to match the sintering shrinkage of anode and electrolyte during the fabrication of single cell pellets. The preparation of BSCF cathode materials has been described elsewhere [33].

2.2. Single fuel cell fabrication

The anode supported single cell was fabricated by a co-pressing and spin coating technique. The anode powder was first placed into a pellet die and pressed into a disc at 20 MPa. Then, SDC electrolyte powder was placed on top and pressed at 250 MPa to produce a bilayer disc. The bilayer disc was fired at 1450 °C for 2 h. BSCF cathode material was mixed with a binder (5 wt.% ethyl cellulose + 95 wt.% terpineol), and the resulting slurry was applied to the top of the electrolyte layer by spin coating using a Laurell WS-400A-6NPP/LITE spin coater, followed by drying at 85 °C for 2 h. The spin coating process was repeated twice to achieve the desired cathode layer thickness. Finally, the coated disc was fired at 1140 °C for 1 h to obtain the single cell pellet. As current collector, Au paste was coated onto both sides. After installation into the flow reactor, the geometric surface area of each side of the single cell was 1.654 cm^2.

2.3. Characterization

The powder X-ray diffraction (XRD) patterns of SDC powder, NiO/SDC powder, and anode powder reduced by H_2 at 700 °C for 3 h were recorded at room temperature using a rotating-anode Rigaku Rotaflex RU-200B series X-ray diffractometer with a Cu-Kα source at 40 kV, 100 mA and scanning rate of 2° min^{-1}.

The anode side of the freshly prepared single cell was reduced by H_2 at 700 °C for 3 h, prior to characterizing the cross-section

morphology of the single cell by an FEI Nova 200 Nanolab SEM/FIB. This instrument was also used to determine the morphology of carbon deposits under high resolution on the single cell anode after testing it for DEO of CH_4.

2.4. Fuel cell test

To measure cell performance, the single cell was mounted in a custom-built flow reactor that allowed to feed 100 sccm dry H_2 or 70 sccm dry CH_4 to the anode side, while compressed air with a flow rate of 350 sccm was fed to the cathode side. The fuel cell tests were carried out in a temperature range from 600 °C to 700 °C under atmospheric pressure. Before performing the corresponding *I–V* measurements, the anode was first reduced in H_2 for 3 h at 700 °C, and then the flow was switched to the fuel gas. The fuel cell *I–V* characteristics were measured using a Powerstat-05 manufactured by Nuvant Systems Inc. In order to study the stability of the single cells, the cells were also operated under 300 mA constant output current for different times (12 h, 24 h, 48 h, and 72 h). After the durability tests, the temperature of the reactor was decreased to room temperature while both the anode and cathode were protected by a flow of 40 sccm Ar. And finally the surface of the tested cell anode was characterized by SEM. To investigate the properties of the deposited carbon species, temperature programmed oxidation mass spectrometry (TPO-MS) was carried out on the tested cell anode/electrolyte bilayer powder using a Micromeritics AutoChem 2910 instrument equipped with a mass spectrometer. To obtain the powder, the cathode layer was first carefully removed by polishing before grinding the remaining material.

3. Results and discussion

3.1. Structural characterization

Fig. 1 shows the XRD patterns of the SDC powder, BSCF powder, NiO/SDC powder, and NiO/SDC reduced by H_2 at 700 °C for 3 h. The SDC powder (curve a) clearly shows a cubic fluorite structure that is essentially identical with the data on the JCPDS 75-0158 standard PDF card. The XRD pattern of the anode powder (curve b) shows diffraction peaks of both SDC and NiO, without any third component peaks. This indicates that there is no chemical reaction between SDC and NiO. After reduction by H_2 (curve c), metallic Ni peaks are present, but there are no peaks attributable to NiO. This demonstrates that H_2 reduction at 700 °C for 3 h is sufficient for complete reduction of NiO in the anode. It also indicates that SDC

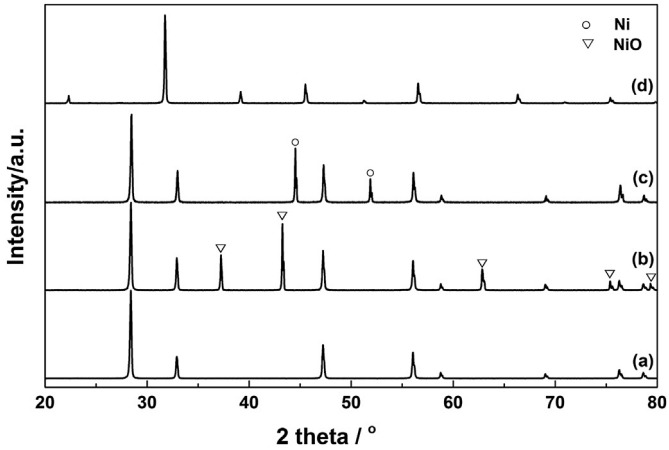

Fig. 1. XRD patterns of the SDC powders (a), NiO/SDC powders (b), reduced NiO/SDC powders (c) and BSCF powders (d).

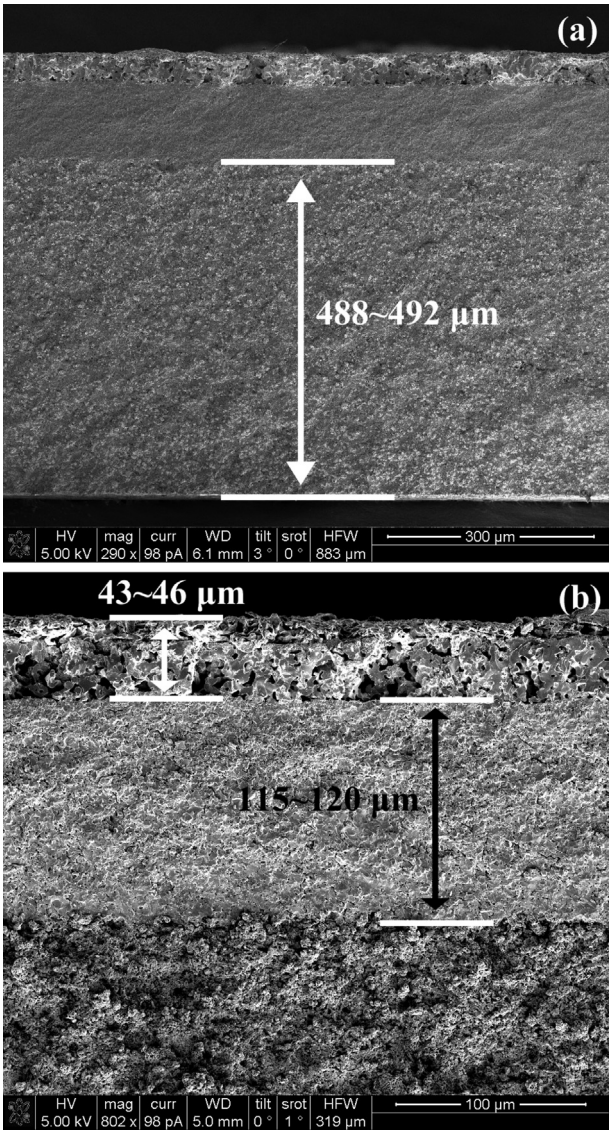

Fig. 2. SEM cross sectional view of the Ni/SDC|SDC|BSCF SOFCs with reduced anode. (a) Lower magnification showing the thickness of the anode layer, (b) Higher magnification showing the thickness of cathode and electrolyte layer.

can retain its structure after this reduction treatment. Therefore, in all the performance tests of single cells, the anode side was exposed to H_2 at 700 °C for 3 h before starting the fuel cell performance measurements. For the BSCF cathode powder, as shown in curve d, a perovskite structure was obtained that matched well with data in the literature [33].

3.2. The microstructure of the single cell

Fig. 2(a) and (b) shows the cross section microstructure of a single cell with reduced anode. The dense SDC electrolyte layer is about 115–120 μm thick and adheres well to the anode substrate, while the thickness of the porous cathode layer is about 43–46 μm. After reduction, the Ni/SDC anode substrate becomes porous and is about 488–492 μm thick.

3.3. Cell performance

The anode supported single cell with the configuration of Ni/SDC|SDC|BSCF was tested using H_2 and dry CH_4 as the fuel,

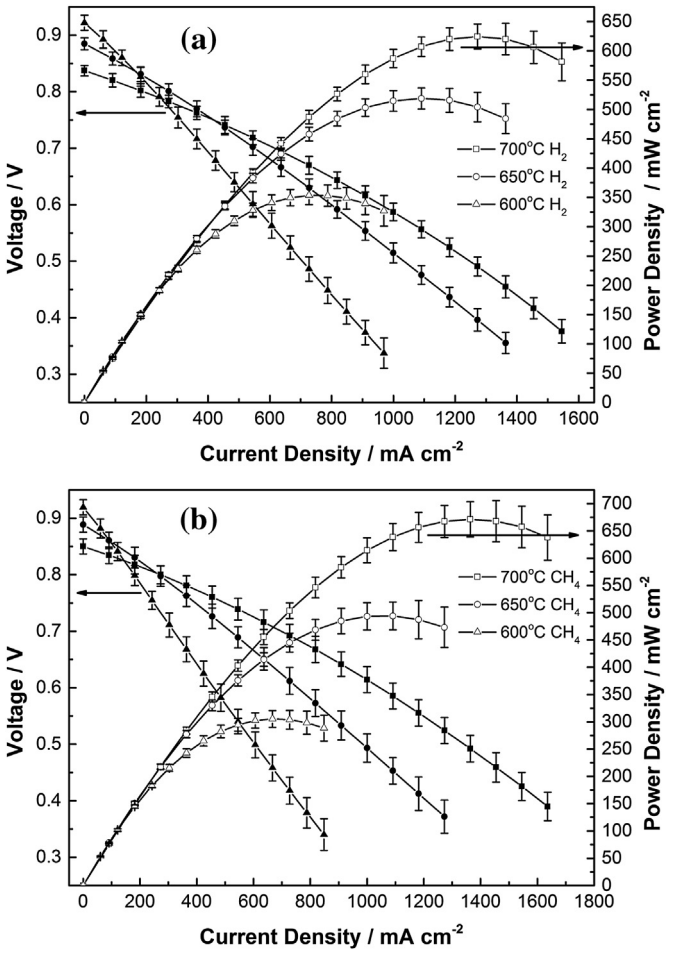

Fig. 3. Voltage and power density as function of current density for Ni/SDC|SDC|BSCF SOFCs in dry H_2 (a) and dry CH_4 (b).

respectively, and compressed air as the oxidant. Fig. 3(a) and (b) shows the performance results obtained from multiple cells under identical configuration and testing procedure.

From Fig. 3(a) and (b), it can be seen that the open circuit voltage (OCV) of the cell for both H_2 as well as CH_4 was lower than the theoretical electromotive force. For instance, the OCV at 700 °C for H_2 was 0.837 V, while the theoretical value is around 1.1 V. For CH_4, the situation becomes more complicated, as both partial electrochemical oxidation (POM) and complete electrochemical oxidation (COM) of CH_4 could occur. The standard electromotive force of POM and COM calculated by Zhang et al. [34] by the Nernst equation were 1.1213 V and 1.0502 V at 700 °C, respectively, which are both higher than the 0.850 V measured in our tests. It is well known that the doped ceria electrolyte exhibits under reducing atmosphere mixed ionic and electronic conduction, which originates from the partial reduction of Ce^{4+} into Ce^{3+} [35]. Therefore, the OCV of a fuel cell with doped ceria electrolyte is usually lower than the theoretical value due to the internal efficiency loss.

Fig. 3(a) shows plots of the voltage and power density as functions of the current density and working temperature for H_2 fuel. The cell exhibited maximum power densities (P_{max}) of 624 mW cm^{-2}, 519 mW cm^{-2}, and 353 mW cm^{-2} at 700 °C, 650 °C and 600 °C, respectively.

For the dry CH_4 fuel, the P_{max} of the single cell reached 671 mW cm^{-2}, 494 mW cm^{-2} and 305 mW cm^{-2} at these temperatures, respectively, as shown in Fig. 3(b). At 700 °C, the cell performance with CH_4 is higher than with H_2, due to the higher energy density of CH_4 and the excellent catalytic activity and stability of Ni/SDC. But at lower temperatures, where the activation of CH_4 is much more difficult to achieve than that of H_2, the performance with H_2 is better. This is in agreement with results from other researchers showing that at high temperatures CH_4 fuel may give a higher power output than H_2 when using good anode materials [36,37].

The stability of the Ni/SDC anode under dry CH_4 fuel was characterized at 600 °C under a constant output current of 300 mA. Fig. 4 shows the plots of output voltage against operation time. As demonstrated in this figure, during 72 h of continuous operation, the output voltage slightly increased at the beginning and then decreased versus time. The slight increase at the beginning is due to the fact that we carried out the stability test by directly changing the fuel cell from OCV condition to the constant output current condition, while recording the data immediately. After the current jump, the cell system needed a short time to stabilize itself. The total performance drop during this 72 h period was only about 3.7%, indicating that the Ni/SDC anode was very stable at 600 °C when operated with dry CH_4 fuel.

There are two major reasons for this stable performance. First, in the Ni/SDC anode, Ni particles are surrounded by the oxygen ion conductor SDC, which can supply oxygen species for the direct electrochemical oxidation of CH_4, and thereby suppress the carbon deposition on Ni particles. And even if some carbon deposits would occur, the oxygen species from SDC can promote their removal, similar to the effects of ceria related materials mentioned in the reforming literature [38–40]. Besides, formation of carbon species from CH_4 by pyrolysis is more favorable at higher temperature [3], while our testing temperature is much lower than that used in SOFCs with YSZ or LSGM electrolytes that typically operate at temperatures higher than 800 °C.

3.4. SEM of tested cell

To investigate the carbon deposition on the anode, the tested cell anode surfaces were characterized by high-resolution SEM. Fig. 5 presents the result for cells after 72 h operation. Only small amounts of carbon species were detected mainly on the Ni surface and at the Ni/SDC interface, but there was no clear evidence of carbon deposition on the SDC surface.

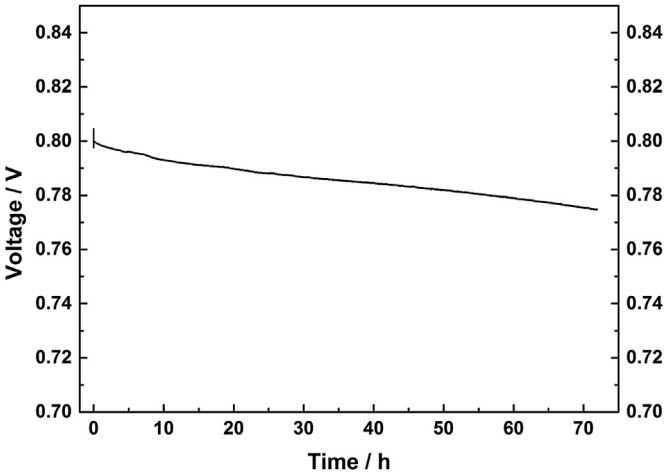

Fig. 4. The long-term performance of Ni/SDC|SDC|BSCF SOFCs in dry CH_4 with a constant 300 mA output current (at 600 °C).

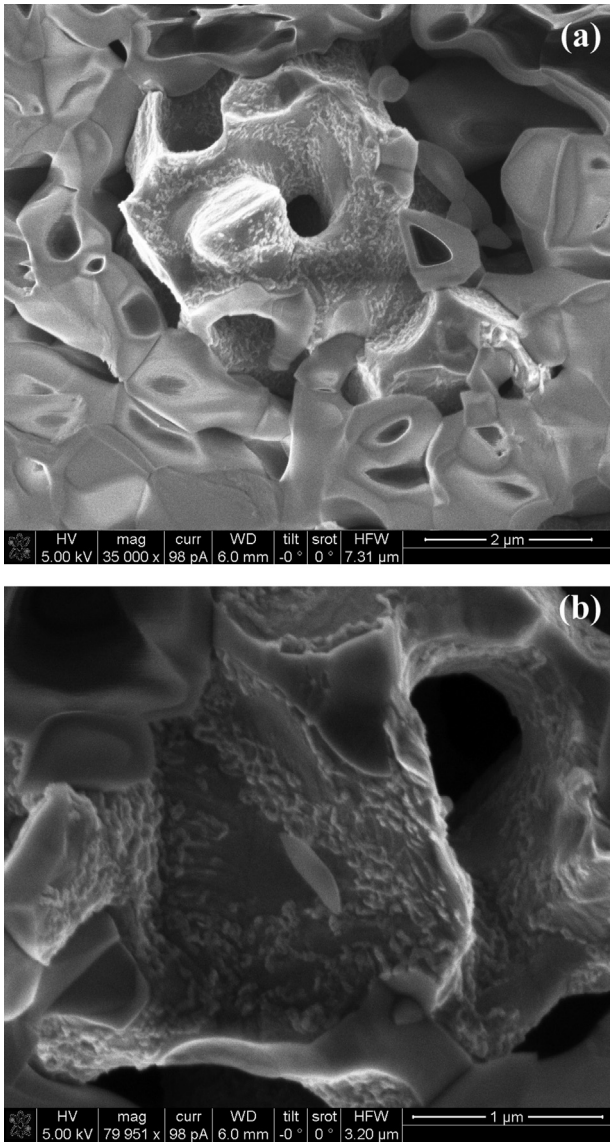

Fig. 5. SEM images of the SOFC anode surface after 72 h stability test. Ni and SDC surface (a), Ni surface (b).

3.5. TPO-MS analysis of carbon deposition

In order to characterize the carbon deposition versus time on stream, TPO-MS analyses were carried out on the ground anode/electrolyte bilayer powders of the tested cell after different operation times (12 h, 24 h, 48 h and 72 h). The powders were first degassed in He for 1 h at 200 °C. After cooling to room temperature, the TPO analysis were carried out in 70 ml min^{-1} 1% O_2/He gas using a ramping rate of 10 °C min^{-1}. As the temperature increased, the various types of carbon reacted with oxygen, giving rise to CO_2 peaks. Fig. 6 shows the normalized carbon dioxide signals (weight of the ground powder normalized to 1 g) for the four different operating times. With increasing operating time, the total amount of carbon formed on the anode increased. However, it must be noted that the CO_2 peaks barely rose above the baseline, and to make them clearly visible, the *y*-axis in Fig. 6 is highly magnified. This indicates that the total amount of carbon deposited was very low in all cases. To further confirm this result, the method developed by Chen et al. [41] was used. Thermogravimetric analysis combined with infrared spectroscopy (TGA–IR) was carried out in 50 ml min^{-1} 21% O_2/N_2 using a Perkin–Elmer TGA-7 coupled to a Perkin–Elmer FT-IR Spectrum 2000. The TGA–IR results showed that there was no visible derivative thermal gravimetric peak and evolved CO_2 IR band related to deposited carbon, indicating that the total amount of carbon was below the detection limits of this TGA–IR process. The fact that the total amount of carbon deposition was very low is in agreement with the very small performance drop during the stability test.

The presence of multiple peaks in the TPO-MS data suggested the existence of different carbon species. In order to reveal the details of the TPO-MS peaks, a multi peak fitting technique was used, and the results are shown by the solid lines in Fig. 6. Four types of carbon species were identified with different peak oxidation temperatures, around 270–280 °C (peak I), 370–390 °C (peak II), 480–500 °C (peak III) and 530–550 °C (peak IV), respectively.

These peaks can be divided into two groups, low temperature peaks (peak I and II) and high temperature peaks (peak III and peak IV). The two low temperature peaks are likely due to the oxidation of poorly polymerized, H-rich carbon or amorphous carbon [42–44], while the high temperature peaks can be attributed to the oxidation of carbon deposited with a higher degree of graphitization, probably filamentous carbon [39]. These findings are in agreement with other literature data about Ni based reforming or partial oxidation catalysts, where the existence of H-rich carbon or amorphous carbon and filamentous carbon has been reported [45,46]. For each group, the difference in oxidation temperature should be due to the difference in the location of the carbon deposit. The lower temperature peaks in each group (peak I and peak III) could be attributed to carbon deposited on the Ni/SDC interface, while the other two peaks (peak II and peak IV) correspond to carbon attached to the Ni surface. The carbon located at the Ni/SDC interface will have a lower oxidation temperature due to high concentration of mobile oxygen vacancies that promote the oxidation of deposited carbon. The fact that the amount of type II carbon is much larger than that of type I also confirms this from another perspective.

The relationship between the amount of different carbon species and operation time is shown in Fig. 7. Type II carbon is the dominant one, and its amount increases with increasing operating time. There are reports stating that filamentous carbon is the cause of degradation for SOFCs with Ni based anode materials [47,48]. When we associate the performance drop with the amount of different kind of carbon deposits, the performance drop shows a clear relationship to the amount of type II and type IV carbon, but the amount of type II carbon is much larger than type IV. Therefore, the formation of type II carbon appears to be the primary reason for the slow performance drop of Ni/SDC anode materials in dry CH_4 fuel.

4. Conclusion

NiO/SDC powders with NiO content of 50 mass% were successfully synthesized by a simple ball milling technique. Anode supported single cells with Ni/SDC as the anode material have been fabricated using SDC and BSCF as the electrolyte and cathode materials, respectively. The single cell exhibited a maximum power density of 671 mW cm^{-2}, 494 mW cm^{-2} and 305 mW cm^{-2} in dry CH_4 at 700 °C, 650 °C and 600 °C, respectively, and the cell performance at 700 °C in CH_4 was better than in H_2. Durability tests were carried out by operation of the cell under a 300 mA constant output current at 600 °C, and only 3.7% performance drop was observed during 72 h operation.

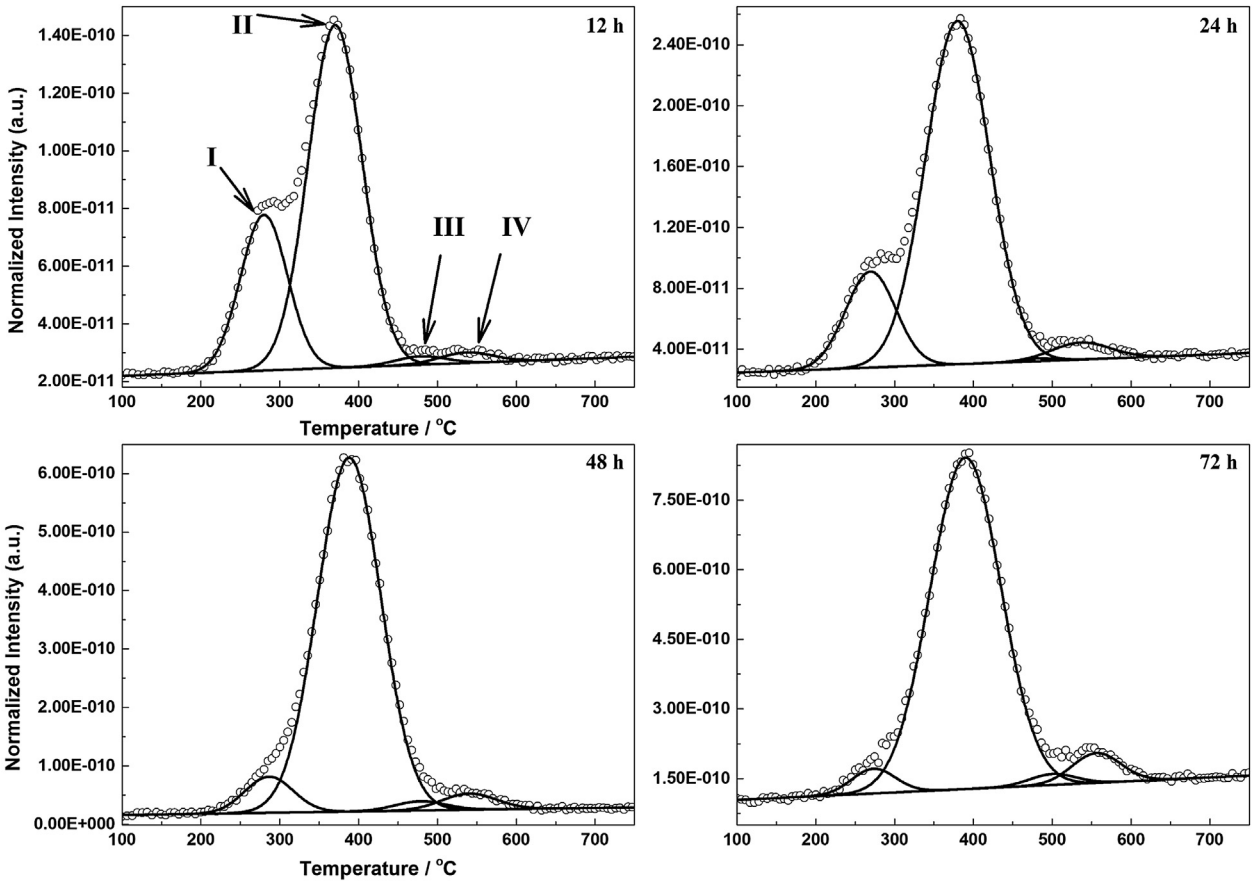

Fig. 6. TPO-MS results for the ground anode/electrolyte bilayer powders of SOFCs after durability test of different durations (o: raw data; solid lines: multi peak fitting results).

The TPO-MS characterization results showed the existence of four different carbon species that were formed on the Ni surface and Ni/SDC interface, but the total amount of deposited carbon was very low. SEM images of the tested cell anode surface also confirmed that carbon mainly formed on the Ni surface and Ni/SDC interface.

All these experimental results indicate that the Ni/SDC material has great potential for use as anode for direct electrochemical oxidation of dry CH_4, especially at low temperatures such as 600 °C.

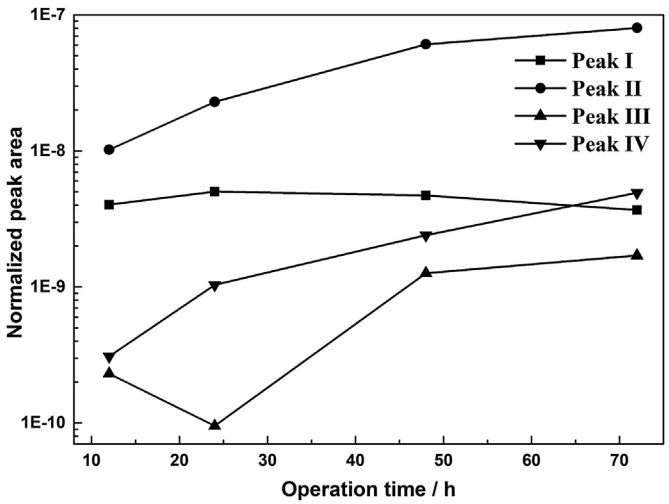

Fig. 7. Amount of different carbon species as function of operation time.

Acknowledgments

Financial support of NSF of China under contract numbers 21076150 and 21120102039 is gratefully acknowledged. The work has also been supported by the Program of Introducing Talents to the University Disciplines under file number B06006, and the Program for Changjiang Scholars and Innovative Research Teams in Universities under file number IRT 0641. The authors acknowledge the use of the FEI Nova 200 Nanolab SEM/FIB instrument in the University of Michigan Electron Microbeam Analysis Laboratory (EMAL) funded by NSF grant #DMR-0320740.

References

[1] A. Lashtabeg, S.J. Skinner, J. Mater. Chem. 16 (2006) 3161–3170.
[2] S.C. Singhal, Solid State Ionics 152–153 (2002) 405–410.
[3] E.P. Murray, T. Tsai, S.A. Barnett, Nature 400 (1999) 649–651.
[4] S.D. Park, J.M. Vohs, R.J. Gorte, Nature 404 (2000) 265–267.
[5] H. Kim, S. Park, J.M. Vohs, R.J. Gorte, J. Electrochem. Soc. 148 (2001) A693–A695.
[6] S. McIntosh, R.J. Gorte, Chem. Rev. 104 (2004) 4845–4865.
[7] L.J. Jia, Y. Tian, Q.H. Liu, C. Xia, J.S. Yu, Z.M. Wang, Y.C. Zhao, Y.D. Li, J. Power Sources 195 (2010) 5581–5586.
[8] A. Atkinson, S. Barnett, R.J. Gorte, J.T.S. Irvine, A.J. Mcevoy, M. Mogensen, S.C. Singhal, J. Vohs, Nat. Mater. 3 (2004) 17–27.
[9] M.D. Gross, J.M. Vohs, R.J. Gorte, J. Mater. Chem. 17 (2007) 3071–3077.
[10] J.W. Yun, S.P. Yoon, H.S. Kim, J. Han, S.W. Nam, Int. J. Hydrogen Energy 37 (2012) 4356–4366.
[11] T. Takeguchi, Y. Kani, T. Yano, R. Kikuchi, K. Eguchi, K. Tsujimoto, Y. Uchida, A. Ueno, K. Omoshiki, M. Aizawa, J. Power Sources 112 (2002) 588–595.
[12] M. Mogensen, K. Kammer, Annu. Rev. Mater. Res. 33 (2003) 321–331.

[13] H. Yokokawa, H. Tu, B. Iwanschitz, A. Mai, J. Power Sources 182 (2008) 400–412.
[14] C.M. Finnerty, N.J. Coe, R.H. Cunningham, R.M. Ormerod, Catal. Today 46 (1998) 137–145.
[15] B.C.H. Steele, Nature 400 (1999) 619–621.
[16] K. Ke, A. Gunji, H. Mori, S. Tsuchida, H. Takahashi, K. Ukai, Y. Mizutani, H. Sumi, M. Yokoyama, K. Waki, Solid State Ionics 177 (2006) 541–547.
[17] M. Ihara, C. Yokoyama, A. Abudula, R. Kato, H. Komiyama, K. Yamada, J. Electrochem. Soc. 146 (1999) 2481–2487.
[18] K. Girona, J. Laurencin, J. Fouletier, F. Lefebvre-Joud, J. Power Sources 210 (2012) 381–391.
[19] M. Pillai, Y.B. Lin, H.Y. Zhu, R.J. Kee, S.A. Barnett, J. Power Sources 195 (2010) 271–279.
[20] R.J. Gorte, H. Kim, J.M. Vohs, J. Power Sources 106 (2002) 10–15.
[21] S. McIntosh, J.M. Vohs, R.J. Gorte, Electrochem. Solid-State Lett. 6 (2003) A240–A243.
[22] H. Kim, C. Lu, W.L. Worrell, J.M. Vohs, R.J. Gorte, J. Electrochem. Soc. 149 (2002) A247–A250.
[23] E. Nikolla, J. Schwank, S. Linic, J. Electrochem. Soc. 156 (2009) B1312–B1316.
[24] Y.B. Lin, Z.L. Zhan, S.A. Barnett, J. Power Sources 158 (2006) 1313–1316.
[25] S.W. Tao, J.T.S. Irvine, Nat. Mater. 2 (2003) 320–323.
[26] S.W. Zha, P. Tsang, Z. Cheng, M.L. Liu, J. Solid State Chem. 178 (2005) 1844–1850.
[27] Y.H. Huang, R.I. Dass, Z.L. Xing, J.B. Goodenough, Science 312 (2006) 254–257.
[28] Y.H. Huang, G. Liang, M. Croft, M. Lehtimaki, M. Karppinen, J.B. Goodenought, Chem. Mater. 21 (2009) 2319–2326.
[29] Y.H. Huang, R.I. Dass, J.C. Denyszyn, J.B. Goodenough, J. Electrochem. Soc. 153 (2006) A1266–A1272.
[30] Z.M. Wang, Y. Tian, Y.D. Li, J. Power Sources 196 (2011) 6104–6109.
[31] H.J. Li, Y. Tian, Z.M. Wang, F.C. Qie, Y.D. Li, RSC Adv. 2 (2012) 3857–3863.
[32] E.D. Wachsman, K.T. Lee, Science 334 (2011) 935–939.
[33] Z.P. Shao, W.S. Yang, Y. Cong, H. Dong, J.H. Tong, G.X. Xiong, J. Membr. Sci. 172 (2000) 177–188.
[34] X. Zhang, S. Ohara, H. Chen, T. Fukui, Fuel 81 (2002) 989–996.
[35] X. Zhang, M. Robertson, C. Deċes-Petit, W. Qu, O. Kesler, R. Maric, D. Ghosh, J. Power Sources 164 (2007) 668–677.
[36] B. Huang, X.F. Ye, S.R. Wang, H.W. Nie, J. Shi, Q. Hu, J.Q. Qian, X.F. Sun, T.L. Wen, J. Power Sources 162 (2006) 1172–1181.
[37] T. Hibino, A. Hashimoto, K. Asano, M. Yano, M. Suzuki, M. Sano, Electrochem. Solid-State Lett. 5 (2002) A242–A244.
[38] R.M. Navarro, M.C. Álvarez-Galván, F. Rosa, J.L.G. Fierro, Appl. Catal. A Gen. 297 (2006) 60–72.
[39] S. Natesakhawat, R.B. Watson, X. Wang, U.S. Ozkan, J. Catal. 234 (2005) 496–508.
[40] Y. Li, X. Wang, C. Xie, C. Song, Appl. Catal. A Gen. 357 (2009) 213–222.
[41] X. Chen, A.R. Tadd, J.W. Schwank, J. Catal. 251 (2007) 374–387.
[42] C.H. Bartholomew, Appl. Catal. A Gen. 212 (2001) 17–60.
[43] J. Chen, X. Yang, Y. Li, Fuel 89 (2010) 943–948.
[44] G. Zeng, Q. Liu, R. Gu, L. Zhang, Y. Li, Catal. Today 178 (2011) 206–213.
[45] S. Wang, G.Q. Lu, Appl. Catal. B 19 (1998) 267–277.
[46] T. Zhu, M. Flytzani-Stephanopoulos, Appl. Catal. A Gen. 208 (2001) 403–417.
[47] H. Kan, H. Lee, Appl. Catal. B 97 (2010) 108–114.
[48] A. Lanzini, P. Leone, C. Guerra, F. Smeacetto, N.P. Brandon, M. Santarelli, Chem. Eng. J. (Lausanne) 220 (2013) 254–263.